HHS Public Access

Author manuscript

Eur J Pharmacol. Author manuscript; available in PMC 2017 July 15.

Published in final edited form as:

Eur J Pharmacol. 2016 July 15; 783: 73–84. doi:10.1016/j.ejphar.2016.04.054.

Cystathionine-γ lyase-derived hydrogen sulfide mediates the cardiovascular protective effects of moxonidine in diabetic rats

Shaimaa S. El-Sayed[a,1], **Mohamed NM. Zakaria**[b], **Rasha H. Abdel-Ghany**[b], and **Abdel A. Abdel-Rahman**[a]

[a]Department of Pharmacology and Toxicology, Brody School of Medicine, East Carolina University, Greenville, NC – 27834

[b]Department of Pharmacology and Toxicology, Zagazig University, Zagazig, Egypt

Abstract

Blunted cystathionine-γ lyase (CSE) activity (reduced endogenous H_2S-level) is implicated in hypertension and myocardial dysfunction in diabetes. Here, we tested the hypothesis that CSE derived H_2S mediates the cardiovascular protection conferred by the imidazoline I_1 receptor agonist moxonidine in a diabetic rat model. We utilized streptozotocin (STZ; 55 mg/kg i.p) to induce diabetes in male Wistar rats. Four weeks later, STZ-treated rats received vehicle, moxonidine (2 or 6 mg/kg; gavage), CSE inhibitor DL-propargylglycine, (37.5 mg/kg i.p) or DL-propargylglycine with moxonidine (6 mg/kg) for 3 weeks. Moxonidine improved the glycemic state, and reversed myocardial hypertrophy, hypertension and baroreflex dysfunction in STZ-treated rats. Ex vivo studies revealed that STZ caused reductions in CSE expression/activity, H_2S and nitric oxide (NO) levels and serum adiponectin and elevations in myocardial imidazoline I_1 receptor expression, p38 and extracellular signal-regulated kinase, ERK1/2, phosphorylation and lipid peroxidation (expressed as malondialdehyde). Moxonidine reversed these biochemical responses, and suppressed the expression of death associated protein kinase-3. Finally, pharmacologic CSE inhibition (DL-propargylglycine) abrogated the favorable cardiovascular, glycemic and biochemical responses elicited by moxonidine. These findings present the first evidence for a mechanistic role for CSE derived H_2S in the glycemic control and in the favorable cardiovascular effects conferred by imidazoline I_1 receptor activation (moxonidine) in a diabetic rat model.

Keywords

imidazoline I_1 receptor; moxonidine; hydrogen sulfide; cystathionine-γ lyase; hypertension; myocardial dysfunction; diabetes

Corresponding Author: Dr. Abdel A. Abdel-Rahman, Department of Pharmacology, Brody School of Medicine, East Carolina University, Greenville, NC 27834, USA, Tel.: +1 252, 744 3470; fax +1 252 744 3203, ; Email: abdelrahmana@ecu.edu

[1]Present address: Department of Pharmacology and Toxicology, Zagazig University, Zagazig, Egypt. shamy_samy84@yahoo.com

1. Introduction

Diabetes predisposes to hypertension and baroreflex dysfunction along with cardiovascular oxidative stress in humans and in experimental animals (Erejuwa et al., 2011; Musial et al., 2013; Shida et al., 2014). Notably, oxidative stress predisposes to hypertension (Yamakawa et al., 2000), and interventions that inhibit oxidative stress (Shida et al., 2014) or sympathetic activity (Ganguly et al., 1986) or enhance nitric oxide (NO) production (Cao et al., 2012; Shida et al., 2014) confer cardiovascular protection. Interestingly, centrally acting imidazoline I_1 receptor agonists (moxonidine and rilmenidine), lower blood pressure (BP) and improve cardiac function, at least partly, via enhanced central and peripheral NO generation (Mukaddam-Daher et al., 2009). On the other hand, much less attention has been given to the potential beneficial cardiovascular effects of another endogenous gaseous cellular modulator, hydrogen sulfide (H_2S), in diabetes in general, and specifically following chronic administration of imidazoline I_1 receptor agonists in diabetic rats.

H_2S, generated by cystathionine-γ-lyase (CSE), cystathionine-β-synthase and 3-mercaptopyruvate sulfur transferase, is suppressed in diabetes (Jain et al., 2010). H_2S confers protection against deleterious consequences associated ischemia/reperfusion injury (Elrod et al., 2007), and hypertension induced myocardial hypertrophy (Huang et al., 2012; Streeter et al., 2013). It is also notable that H_2S alleviates myocardial dysfunction associated with insulin resistance (Hu et al., 2014), and improves glycemic control in diabetic rats (Xue et al., 2013b). Importantly, imidazoline I_1 receptor agonists inhibit sympathetic outflow to the heart and vasculature (Honda et al., 2013), and in obese hypertensive subjects, sympathetic inhibition ameliorates insulin resistance (Esler et al., 2006). Notably, despite common signaling cascades triggered by imidazoline I_1 receptor activation (Mukaddam-Daher et al., 2009) and H_2S (Hua et al., 2013), there are no reports on two possible mechanisms by which endogenous H_2S might mediate the anti-inflammatory and the favorable glycemic and cardiovascular effects of imidazoline I_1 receptor agonists in diabetes. First, low H_2S is linked to lower levels of the anti-inflammatory peptide adiponectin (Jain et al., 2012), and reductions in adiponectin contribute to oxidative stress in diabetes (Akiyama et al., 2010; Liu et al., 2015). Second, it is possible that the favorable cardiovascular and antioxidant effects of H_2S involve suppression of the death associated protein kinase-3 (DAPK3), an upstream activator of mitogen activated protein kinases (MAPKs), which are implicated in oxidative stress and hypertrophy in hypertension (Usui et al., 2012).

In this study, we tested the hypothesis that enhanced generation of cellular H_2S underlies the favorable cardiovascular and glycemic effects of moxonidine in a rodent model of diabetes. To test this hypothesis, we conducted integrative cardiovascular and molecular/biochemical studies in STZ (55 mg/kg) diabetic rat model, and employed two doses of moxonidine to determine if the drug effects were dose-dependent. Finally, we elucidated the mechanistic role of the CSE-derived H_2S in the I_1-mediated effects by investigating the ability of the H_2S synthesis inhibitor DL-propargylglycine to abrogate the favorable cardiovascular and glycemic effects caused by moxonidine in STZ diabetic rats.

2. Materials and methods

2.1. Animals

Male Wistar rats (225–250 g, Charles River Laboratories, Raleigh, NC), were used in the present study. Rats were housed individually in standard plastic cages upon starting treatment and allowed free access to water and Purina chow (St. Louis, MO). Rats were maintained on a 12–12-hr light-dark cycle with light automatically turned off at 7:00 p.m. and the temperature was maintained at 22±1°C. All procedures were approved by the institutional animal care and use committee and conducted in accordance with the Guide for the Care and Use of Laboratory Animals as adopted by the U.S. National Institute of Health, and the Update of the Guide for the Care and Use of Laboratory Animals. et al., 2011).

2.2. Induction of diabetes

One week after arrival, rats were fasted overnight (~16 h) and received freshly prepared STZ (55 mg/kg i.p) in 0.1 M citrate buffer (pH 4.0) or the buffer (control). Drinking water was replaced with 5% dextrose on the day of STZ injection, and 2 days later blood glucose level (BGL) was measured by a Blood Glucose Monitoring System (ReliOn®, Prime). Onset of diabetes was identified by polydipsia, polyuria and BGL >250 mg/dl. Rats that exhibited those characteristics were considered diabetic, and buffer-treated rats were used as non-diabetic controls as reported (Liang et al., 2013).

2.3. Protocols and experimental groups

In accordance with the timeline depicted in Fig. 1, four weeks after STZ injection, 3 groups of rats (n=5–9 each) were housed individually and received daily moxonidine (2 or 6 mg/kg; gavage) or the moxonidine vehicle (0.2% tween 80 in saline). One group of rats (n=8), which received citrate buffer (vehicle for STZ), also received daily saline injection and served as nondiabetic control. Moxonidine or its vehicle was administered for 3 weeks according to reported dose regimen (Henriksen et al., 1997).

In order to test the hypotheses that endogenous H_2S confers favorable cardiovascular and glycemic effects, and mediates the cardioprotection and glycemic control conferred by imidazoline I_1 receptor activation (moxonidine) in STZ diabetic rats, two groups of nondiabetic rats (injected with citrate buffer) and three groups of STZ-treated diabetic rats (n=5–9 each) were employed 4 weeks after STZ or vehicle injection. The two nondiabetic rat groups received daily i.p saline (1 ml/kg) (nondiabetic control) or DL-propargylglycine (37.5 mg/kg; i.p) (nondiabetic+DL-propargylglycine) injections. One of the 3 diabetic groups received daily i.p. saline (vehicle for DL-propargylglycine) and 0.2% tween 80/saline p.o. (vehicle for moxonidine) and served as diabetic control group. The remaining two diabetic groups received daily DL-propargylglycine (37.5 mg/kg; i.p) along with moxonidine or its vehicle. Drug doses were based on reported studies (Henriksen et al., 1997; Yan et al., 2004). In all groups, daily drug or vehicle administration continued for 3 weeks after which the hemodynamic and biochemical studies were conducted as described in the following sections.

2.4. Body and heart weight changes

Body weights were determined on the day of, and weekly for 3 weeks after STZ or vehicle administration. On the day of surgery, body weights were determined, and at the conclusion of the cardiovascular measurements, the rats were euthanized, the hearts were excised, washed with ice-cold saline, weighed, and stored at −80°C for subsequent biochemical studies (see below). The collected data were used to calculate heart weight (HW) to body weight (BW) ratio for each rat as reported (Lee et al., 2008).

2.5. Oral glucose tolerance test (OGTT)

Two days before the conclusion of the study, OGTT was performed following overnight fast (~16 h). A Blood Glucose Monitoring System (ReliOn®, Prime) was used to measure BGL before and 4 times at 30 min intervals after oral administration of 10% glucose solution (1 g/10 ml/ kg) as reported (Frankenfeld et al., 2014).

2.6. Intravascular and left ventricular catheterization

Rats were anesthetized with i.p injection of ketamine (9 mg/100g) and xylazine (1 mg/ 100g). As described in our previous studies (El-Mas and Abdel-Rahman, 2014), a catheter consisting of 5 cm PE-10 tubing bounded to 15 cm PE-50 tubing was placed in the abdominal aorta via left femoral artery and a PE-50 tubing was inserted into the left ventricle through the carotid artery for the measurement of arterial blood pressure (BP) and left ventricular function, respectively. Measurements of left ventricular function using this method were verified against the use of a Millar catheter in our reported studies. Catheters were then tunneled subcutaneously and exteriorized at the back of the neck between the scapulae. Catheters were flushed with heparinized saline and plugged by stainless-steel pins. Incisions were closed with surgical clips and swabbed with Povidone-iodine solution. After surgery, each rat received s.c injections of analgesic, buprenorphine (Buprenex, 0.03 mg/kg, Reckitt Benckiser, Richmond, VA), and penicillin G procaine and penicillin G benzathine (Durapen, 100,000 U/kg, Vedco Inc., Over Land Park, KS).

Left ventricular pressure and BP measurements after the rats fully regained consciousness. The arterial and left ventricular catheters were connected to pressure transducers, BP and left ventricular pressure were recorded by a ML870 powerlab 8/30 (ADInstruments, Colorado Springs, CO) and analyzed by Lab-Chart Pro (Version 7) software (ADInstruments). After stabilization, the average of 30 min measurements of BP, heart rate (HR) and left ventricular function indices were obtained from treatment and control groups (Fig. 1). Heart rate (HR) and the maximum rate of pressure change in the ventricle ($LV+dp/dt_{max}$) were extracted from BP and Left ventricular pressure recordings, respectively by the Lab-Chart (Version 7) blood pressure analysis module as in our reported studies (El-Mas and Abdel-Rahman, 2014).

2.7. Baroreflex sensitivity (BRS) analysis by sequence method

Spontaneous BRS was calculated using Nevrocard SA-BRS, software package for BRS analysis in small animals as in our previous studies (Shaltout and Abdel-Rahman, 2005). This sequence method is based on quantification of at least three beats in which systolic arterial pressure consecutively increases (UP) or decreases (Down) along with changes in

the R-R interval of the subsequent beat in the same direction. Overall, three parameters were obtained by this method, sequential BRS UP, DOWN (data not shown) and total (Shaltout and Abdel-Rahman, 2005).

2.8. Blood and tissue collection

At the conclusion of hemodynamic measurements, blood was collected in heparinized or non-heparinized tubes and centrifuged at 2040 g for 12 min; the plasma or serum were collected, respectively, and divided into aliquots. Rats were then euthanized; hearts were collected and flash frozen in 2-methylbutane (Sigma-Aldrich, St. Louis, MO) in dry ice. Plasma and serum aliquots and tissues were stored at −80°C until being processed for biochemical studies.

2.9. Western blot analysis

Ventricular tissues were homogenized on ice in lysis buffer containing 20 mM Tris, pH 7.5, 150 mM NaCl, 1mM EDTA, 1 mM EGTA, 1 % Triton X-100, 2.5 mM Sodium pyrophosphate, 1 mM β-glycerolphosphate, 1 mM activated sodium orthovanadate and 1 μg/ml leupeptin with protease inhibitor cocktail (Roche diagnostics, Indianapolis, IN). After centrifugation (12000 g for 10 min), proteins in the supernatant was quantified by using Bio-Rad protein assay system (Bio-Rad Laboratories, Hercules, CA). Protein extracts (60–120 μg/lane) were run on 8% or 12% SDS PAGE by electrophoresis at 125 V (Bio-Rad Laboratories, Hercules, CA(. Gels were electroblotted to nitrocellulose membranes via semidry transfer using the Bio-Rad Transblot SD transfer cell (Bio-Rad Laboratories, Hercules, CA) at 25 V for 30 min. The nitrocellulose membranes were then incubated for 2–3 h in Odyssey Blocking Buffer (LI-COR Bioscience, Lincoln, NE) to reduce nonspecific bands. After blocking membranes were incubated at 4°C overnight with the mouse anti-nischarin for imidazoline I_1 receptor (Santa-Cruz biotechnology, Dallas, TX, 1:500), rabbit anti-cystathionase “anti-CSE” (Abcam, Cambridge, MA, 1:1000), rabbit anti-P38 MAPK (Cell signaling, Beverly, MA, 1:500), mouse anti-Phospho-p38 MAPK (Thr180/Tyr182) (Cell signaling, Beverly, MA, 1:500), rabbit anti-ERK1/2 (Cell signaling, Beverly, MA, 1:500), mouse anti-Phospho-ERK1/2 (Cell signaling, Beverly, MA, 1:200) and rabbit anti-DAPK-3 (Cell signaling, Beverly, MA, 1:500). Mouse anti-GAPDH (Abcam, Cambridge, MA, 1:15k) or rabbit anti-GAPDH (Trevigen, Gaithersburg, MD, and 1:10k) was used for GAPDH the loading control. Each antibody was diluted in Odyssey Blocking Buffer (LI-COR Bioscience, Lincoln, NE) with 0.1 % tween.

On the next day, the blots were washed with 0.1 % phosphate buffered saline-tween (PBST) 3 times, 10 min each, then incubated with fluorescently labeled secondary antibody, goat anti-mouse and goat anti-rabbit (1:15000, LI-COR Bioscience, Lincoln, NE) diluted in Odyssey Blocking Buffer (LI-COR Bioscience, Lincoln, NE) with 0.1 % tween, for 1 hr. at room temperature. At end of incubation period, membranes were gone through 2 additional washes with PBST and one with PBS, and then membranes were placed in PBS and were taken for imaging. Imaging acquisition was performed via the Odyssey Infrared Imaging System (LI-COR Bioscience). Protein bands were quantified by integrated intensities using Odyssey Infrared Imaging Software (Version 3.0, LI-COR Bioscience), normalized to GAPDH and expressed in arbitrary units.

2.10. Immunohistochemical analysis

Following the same protocol as in our previous study (Wang and Abdel-Rahman, 2002), ventricular tissues were fixed in 4% paraformaldehyde-PBS solution for 4 h at 4°C. The tissues were then transferred to 20% sucrose-PBS solution and incubated for 48 h at 4°C. The sucrose infiltrated tissues were frozen and sectioned. Cryostat sections (10 μm in thickness) were immunostained with mouse anti-CSE (Abcam, Cambridge, MA) or rabbit anti-DAPK-3 (Cell signaling, Beverly, MA) using a modification of the avidin-biotin complex method (ABC). An ABC kit (Vector laboratories, Burlingame, CA) was used to perform immunohistochemistry. Briefly, sections were incubated serially with the following solutions: (1) 0.1% H_2O_2 for 30 min to block endogenous peroxidase activity, (2) normal animal serum solution containing 0.4% Triton X-100 for 1 h to reduce nonspecific binding, (3) primary antibody against CSE (1:200) or DAPK-3 (1:200) solution for 48 h at 4°C, (4) diluted biotinylated secondary antibody solution for 1 h at 4°C, (5) ABC reagent solution for 30 min at room temperature, (6) peroxidase substrate solution until the desired stain intensity developed then clear and mount. PBS (pH 7.4) was used to dilute each solution and to wash the sections 3 times after each step.

2.11. Measurement of myocardial H_2S synthesizing enzyme activity

Myocardial H_2S synthesizing enzyme activity was determined as described (Stipanuk and Beck, 1982). Briefly, left ventricular tissues were homogenized in ice-cold 50 mM potassium phosphate buffer (pH 6.8). After centrifugation (12000 g for 10 min), the protein in the supernatant was quantified by Bio-Rad protein assay system (Bio-Rad Laboratories, Hercules, CA). Add 100 μl sample (200 μg protein) to 900 μl of the reaction mixture (100 mM potassium phosphate buffer “pH 7.4”, 10 mM L-cysteine and 2 mM pyridoxal 5′-phosphate). Cryovial tube (2 ml) were used as center wells for each bottle, each tube contained 0.5 ml of 1 % zinc acetate as trapping solution and a filter paper of 1×1.5 cm2 to increase the air-to-liquid contact surface. The bottles were flushed with N2 before being sealed with double layer of parafilm. The reaction was started by transferring the bottles to a 37°C shaking water bath and incubated for 90 min. At the end of incubation period, 500 μl of 50% trichloroacetic acid was added to the reaction mixture to stop the reaction; the bottles were sealed again and re-incubated in a 37°C shaking water bath for another 60 min to ensure complete trapping of all H_2S released from the reaction. Subsequently, the contents were transferred into Eppendorff tubes and the following reagents were added: 134 μl of 20 mM N, N dimethyl p-phenylenediamine sulfate and 134 μl of 30 mM Iron (III) chloride (FeCl3). The mixture was then incubated for 20 min at room temperature, and contents were transferred into 96 well plate and read at 650 nm in a microplate reader. The H_2S concentrations were calculated against a calibration curve of the standard NaHS solution in 50 mM potassium phosphate buffer, pH 6.8 (0–320 μM NaHS equivalent to 0–96 μM H_2S as H_2S concentration was calculated as 30% of the NaHS concentration in the calculation (Velasco-Xolalpa et al., 2013)). Myocardial H_2S enzyme synthesizing activity was expressed as nmol/mg protein/min.

2.12. Measurement of myocardial Nitric oxide (NO)

Nitric oxide (NO) measurement was conducted in myocardial tissues from rats of different experimental groups using commercial Nitrate/Nitrite Colorimetric Assay kit according to manufacturer's instructions (Cayman Chemical, Ann Arbor, MI).

2.13. Measurement of serum adiponectin

The serum circulated adiponectin was measured using commercial Mouse/Rat adiponectin ELISA kit according to manufacturer's instructions (B-Bridge International Inc., Cupertino, CA).

2.14. Measurement of oxidative stress (expressed as malondialdehyde "MDA")

As an indicator of oxidative stress, MDA measurement was conducted in both plasma and myocardial tissues from rats of different experimental groups using commercial TBARS (TCA) Assay kit according to manufacturer's instructions (Cayman Chemical, Ann Arbor, MI).

2.15. Drugs and Chemicals

Moxonidine (American Custom Chemicals Corp., San Diego, CA), DL-propargylglycine (Chem-Impex International Inc., Wood Dale, IL), N,N dimethyl P-phenylene diamine sulfate (Acros Organics "Thermo Fischer Scientific", Bridgewater, NJ), TEMED (Thermo scientific, Rockford, IL), Acrylamide 40% solution (Fischer Scientific, Pittsburg, PA), ammonium persulfate (J.T Baker, Center Valley, PA), heparin (Elkins Sinn Inc., Cherry Hill, NJ) and sterile saline (B. Braun Medical Inc., Bethlehem, PA) were purchased from commercial vendors. All other chemicals were purchased from Sigma-Aldrich.

2.16. Data analysis and statistics

Values are expressed as mean ± S.E.M. Statistical analysis were conducted by using one-way or repeated measures analysis of variance with Bonferroni post hoc test and student's t-test. Prism 5.0 software (Graphpad Software Inc., San Diego, CA) was used to perform statistical analysis, $P<0.05$ was considered significant.

3. Results

3.1. Cystathionine-γ synthase (CSE) inhibitor (DL-propargylglycine) exacerbates weight loss and cardiac hypertrophy induced by diabetes

During the 7-week study, body weight gain was recorded and at the conclusion of the study heart weight/body weight ratio (HW/BW) was calculated to evaluate cardiac hypertrophy. Compared with non-diabetic rats, STZ-treated diabetic rats exhibited significantly ($P<0.05$) lower BW and higher HW/BW ratio (Table 1). Moxonidine caused dose-dependent exacerbation of the STZ-associated reduction in gain in BW and, and this effect was further exacerbated ($P<0.05$) by the CSE inhibitor "DL-propargylglycine" (Table 1). Comparison of HW/BW ratios revealed that the diabetes- induced cardiac hypertrophy was reversed by moxonidine, but persisted in DL-propargylglycine treated diabetic rats (Table 1).

3.2. CSE inhibition attenuates moxonidine-evoked improvement of glycemic control in diabetic rats

Oral glucose tolerance test (OGTT) conducted 7 weeks after STZ or vehicle injection, in the absence or presence of the daily pharmacologic intervention during the last 3 weeks, showed that: (i) STZ-treated rats exhibited substantially ($P<0.05$) higher fasting blood glucose level (BGL) (Fig. 2C), and a compromised glycemic control (Fig. 2A, B). (ii) Moxonidine dose-dependently reversed these effects (Fig. 2). (iii) CSE inhibition (DL-propargylglycine) had no effect on fasting BGL or OGTT outcomes in nondiabetic rats, but significantly ($P<0.05$) attenuated the favorable glycemic control conferred by moxonidine (Fig. 2).

3.3. CSE inhibition abrogates moxonidine-induced improvement of hemodynamic function and baroreflex sensitivity (BRS) in STZ-diabetic rats

At the conclusion of the seven weeks following STZ/vehicle injection, and in the presence or absence of daily pharmacologic intervention during the last 3 weeks, left ventricular indices and blood pressure (BP; recorded and analyzed by lab-chart Pro software), and spontaneous baroreflex sensitivity (BRS; calculated using Nevrocard SABRS software) were recorded in all treatment and control rats. Diabetic rats exhibited significant ($P<0.05$) elevation in BP and significant ($P<0.05$) reductions in maximum rate of left ventricle pressure rise (LV $+dp/dt_{max}$) and cardiac baroreflex function (Table 2). Moxonidine reversed these diabetes-evoked deleterious effects, and the higher dose (6 mg/kg) resulted in further reduction in BP and heart rate (Table 2). These favorable cardiovascular and baroreflex effects of moxonidine were abrogated ($P<0.05$) by concurrent H_2S inhibition with DL-propargylglycine (Table 2).

3.4. Moxonidine reverses diabetes-evoked reductions in myocardial CSE expression/activity, hydrogen sulfide (H_2S) and nitric oxide (NO) levels

At the conclusion of hemodynamic measurements, the hearts were collected for the measurements of imidazoline I_1 receptor expression, CSE expression/activity, H_2S and NO level in all treatment and control groups. These ex vivo studies revealed significant ($P<0.05$) elevations in imidazoline I_1 receptor expression (Fig. 3A) and reductions ($P<0.05$) in CSE expression and activity (Fig. 3B, C) and in H_2S and NO levels (Fig. 5A, B) in the myocardium of STZ diabetic rats. The higher moxonidine dose reversed these molecular responses (Figs. 3A, B, C and 5A, B), and these favorable effects of moxonidine were abrogated ($P<0.05$) by concurrent CSE inhibition with DL-propargylglycine (Figs. 3–5).

3.5. CSE-inhibition (DL-propargylglycine) abrogates moxonidine-induced attenuation of oxidative stress mediators in myocardia of STZ-diabetic rats

Mediators of myocardial oxidative stress (p38, ERK 1/2 and DAPK-3) were measured in all treatment and control groups. These ex vivo studies revealed significant ($P<0.05$) elevations in phosphorylation of p38 and ERK1/2 (Fig. 6A, B) in the myocardium of STZ diabetic rats. The higher moxonidine dose reversed these molecular responses (Figs. 6A, B), and significantly ($P<0.05$) suppressed DAPK3 expression (Fig. 6C, Fig. 7). These favorable effects of moxonidine were abrogated ($P<0.05$) by concurrent CSE inhibition with DL-propargylglycine (Fig. 6, 7).

3.6. CSE-inhibition aggravates diabetes – induced adiponectin reduction and oxidative stress elevation

Diabetic rats exhibited substantially ($P<0.05$) lower serum adiponectin (Fig. 8A) and significantly ($P<0.05$) elevated myocardial and plasma MDA (index of oxidative stress) levels (Fig. 8B, C). Moxonidine (6 mg/kg) partially restored serum adiponectin (Fig. 8A), and reversed the elevations in myocardial (Fig. 8B) and plasma (Fig. 6C) MDA levels in diabetic rats. The reduction in adiponectin and elevation of MDA levels persisted in DL-propargylglycine-treated diabetic rats (Fig. 8). Finally, concurrent CSE inhibition (DL-propargylglycine) abrogated ($P<0.05$) the favorable effects of moxonidine on adiponectin in diabetic rats (Fig. 8A), which paralleled similar abrogation, by CSE inhibition, of the favorable glycemic (Fig. 2), antioxidant (Figs. 3, 5 and 6), and hemodynamic (Table 2) effects conferred by moxonidine in diabetic rats.

4. Discussion

The molecular mechanisms of the imidazoline I_1 receptor-mediated cardioprotection in experimental diabetes remain unknown. We tested the novel hypothesis that moxonidine ameliorates the glycemic and hemodynamic anomalies in the STZ-diabetic rat model by activating the cystathionine-γ lyase (CSE)/H_2S system. The most important findings of this study in STZ rats are: (1) moxonidine reversed the myocardial dysfunction, hypertension, and the impaired glycemic control; (2) moxonidine reversed the suppressions in myocardial CSE expression, H_2S and NO and serum adiponectin level, and restored myocardial redox state; (3) CSE inhibition (DL-propargylglycine) abrogated the favorable cardiovascular, glycemic and antioxidant effects of moxonidine. Collectively, these pharmacological and molecular and findings implicate endogenous H_2S in the favorable cardiovascular and glycemic effects of imidazoline I_1 receptor activation in diabetes (Fig. 9).

STZ-treated rats exhibited diabetes-related features such as suppressed gain in body weight (BW), hyperglycemia and impaired glycemic control (Patel et al., 2011; Zheng et al., 2006). The suppressed gain in BW was exacerbated by pharmacological interventions that improved (moxonidine) or worsened (DL-propargylglycine) glycemic control (Table 1), which rules out the dependence of glycemic control on gain in BW in our model system. The moxonidine-evoked reduction in BW gain agrees with findings in obese spontaneously hypertensive rats (SHR) (Bing et al., 1999). Here, we present the first evidence for a favorable moxonidine effect on glycemic control in a diabetic rat model (Fig. 2A–C), which might involve central sympathoinhibition (Rosen et al., 1997) or enhancement of glucose uptake by skeletal muscles (Ernsberger et al., 1999). Further, we present new findings in support of H_2S contribution to the moxonidine-evoked favorable glycemic control in diabetic rats.

Moxonidine reversal of the impaired glycemic control (Fig. 2A, B, C) and the associated reductions in myocardial CSE expression and H_2S levels (Figs. 3B, 4 and 5A), in diabetic rats, suggest a causal role for endogenous H_2S in moxonidine effects. This conclusion is supported by the reversal of insulin resistance by H_2S donors (Xue et al., 2013b), and the protective role of CSE against glucotoxicity and development of diabetes (Okamoto et al., 2013). Next, our findings suggest that moxonidine improvement of glycemic control, and

cardiovascular function (see below), in diabetic rats involves, at least partly, H_2S-dependent generation of the anti-inflammatory adipokine adiponectin because: (i) the diminished adiponectin level in diabetic rats (Fig. 8A) agrees with findings in experimental (Akiyama et al., 2010) and clinical (Ebinc et al., 2008) diabetes; (ii) restoration of adiponectin by moxonidine (Fig. 8A), which agrees with a clinical finding (Ebinc et al., 2008), was paralleled with elevations in CSE expression/activity and H_2S levels (Figs. 3B, C, 4 and 5A); (iii) concomitant CSE/H_2S inhibition (DL- propargylglycine), which suppresses adiponectin in adipocytes (Manna and Jain, 2012), abrogated restorations of adiponectin (Fig. 8A) and CSE/H_2S (Figs. 3B, C, 4 and 5A) as well as the improvement of glycemic control (Fig. 2B) caused by moxonidine in STZ rats.

The STZ diabetic rats exhibited modest elevation in BP (Table 2), which agrees with an increase (Bunag et al., 1982; Musial et al., 2013), but not with a no-change (Zheng et al., 2006) or a reduction (Borges et al., 2006; Leung and Pang, 2014) in BP in STZ-rats. Such variability might be explained by differences in the responses of the major determinants of BP. For example, the hyperglycemia (Fig. 2B) induction of osmotic diuresis (Abe et al., 2002), and oxidative stress (Saini et al., 2014), which suppresses myocardial function in STZ rats (Table 2), might ultimately, lower BP. By contrast, the sympathoexcitation caused by hyperglycemia-evoked neuronal oxidative stress (Patel et al., 2011), and the baroreflex dysfunction shown here (Table 2) and in some (Milan et al., 2007), but not in other (Patel and Zhang, 1995) studies, might tip the balance towards the slight elevation in BP in STZ rats (Table 2). The latter might also result from reduced NO synthesis, caused by persistent hyperglycemia, reported here (Fig. 5B) and in reported studies (Ibrahim et al., 2005; Pieper, 1998). By the same token, the enhanced peripheral and central NO generation (Mukaddam-Daher et al., 2009), the central sympathoinhibition (Ernsberger et al., 1999; Honda et al., 2013; Li and Abdel-Rahman, 2007) as well as the improvement of baroreflex function here (Table 2), and in reported studies (Turcani, 2008), might contribute to moxonidine-evoked hypotension in STZ rats. Collectively, these findings might explain the modest BP elevation and its reversal by moxonidine in STZ rats in the present study.

Our multilevel approach supports our hypothesis that the parallel reductions in H_2S, which serves antioxidant role (Xue et al., 2013a), and in the antiinflammatory hormone adiponectin (Fig. 8A) adversely influence the myocardial redox state and function. Equally important, we present evidence that reversal of these adverse biochemical events play a mechanistic role in the salutary cardiovascular effects of moxonidine in diabetes. Consistent with a reduced plasma H_2S levels in diabetic SHR (Ahmad et al., 2012), myocardial CSE expression/activity and H_2S content were significantly reduced (Fig. 3B, C and 5A) along with a myocardial dysfunction (Table 2) in STZ rats. Further, moxonidine amelioration of myocardial dysfunction (Table 2) in STZ diabetic rats was associated with restorations of CSE activity/H_2S (Figs. 3C and 5A) and adiponectin (Fig. 8A) and MDA levels (Fig. 8B, C) towards control levels. The moxonidine-evoked MDA suppression (Fig. 8B, C) agrees with reported findings following brain ischemia (Gupta and Sharma, 2014). Finally, pharmacologic inhibition of CSE activity, which abrogated moxonidine ability to restore H_2S (Fig. 5A) and adiponectin (Fig. 8A) levels, also abrogated the salutary cardiac effect of moxonidine (Table 2) in STZ diabetic rats.

We report the first myocardial imidazoline I_1 receptor upregulation in diabetic rats (Fig. 3A). This finding, which extends similar findings in hypertension and heart failure (El-Ayoubi et al., 2002; Stabile et al., 2011), might reflect a compensatory response against oxidative stress for the following reasons. First, the enhanced p38 (Fig. 6A) and ERK1/2 (Fig. 6B) phosphorylation agrees with findings in models of diabetes (Jiang and Steinle, 2010; Li et al., 2012), and high fat diet (Qi et al., 2013). Although others reported no change in p38 phosphorylation in diabetic heart (Jiang and Steinle, 2010), it is important to note that phosphorylated MAPKs are implicated in myocardial oxidative stress and dysfunction (Jiang and Steinle, 2010; Li et al., 2012; Qi et al., 2013). Consistent with this premise, moxonidine reversed oxidative stress and increased adiponectin (Fig. 8) along with normalizing MAPK phosphorylation (Fig. 6A, B), which may counteract the compensatory increase in myocardial imidazoline I_1 receptor expression in moxonidine-treated diabetic group (Fig. 3A). These findings in STZ rats are supported by similar responses caused by chronic moxonidine administration in other model systems including SHRs and cardiomyocytes (Aceros et al., 2011; El-Ayoubi et al., 2004; Ernsberger et al., 1999; Hamilton et al., 1993; Mukaddam-Daher, 2012). Second, we present a novel molecular mechanism for the favorable cardiovascular and redox effects of moxonidine in diabetes based on recent evidence that identified DAPK3 as an upstream activator of MAPKs, and as a mediator of oxidative stress and hypertension (Usui et al., 2012). In agreement with the ability of a selective pharmacological inhibitor of DAPK3 to reduce vascular hypertrophy, oxidative stress, BP and vascular DAPK3 level in hypertensive rats (Usui et al., 2012), moxonidine reduced myocardial DAPK3 expression (Fig. 6C, 7), myocardial hypertrophy (Table 1), oxidative stress (Fig. 8C) and BP (Table 2) in diabetic rats. These moxonidine-evoked molecular responses are dependent on CSE/H_2S signaling because they were abrogated by concurrent CSE inhibition by DL-propargylglycine (Fig. 3, 4).

It is important to comment on the following limitations of our study. First, the imidazoline I_2 receptor might contribute to moxonidine evoked glycemic control (Chen et al., 2011). Therefore, future studies using selective imidazoline receptor antagonists are needed to discern the roles of both receptor subtypes in this phenomenon. Second, we did not include control rats treated with moxonidine. While this issue deserves future investigation, it is notable that studies on the cardiovascular effects of moxonidine in rodent models of other pathological conditions (hypertension) did not include control rats treated with moxonidine (Van Kerckhoven et al., 2000) because moxonidine-like drugs do not lower BP in conscious normotensive rats (Abdel-Rahman, 1992). Third, although moxonidine doses were selected based on reported studies (Henriksen et al., 1997), caution is needed in future studies when using the higher dose due to the marked drop in BP and HR. Fourth, when used in reported doses (Yan et al., 2004) for the first time in STZ diabetic rats, DL-propargylglycine had no effect on H_2S or adiponectin (Figs. 5A and 8A) levels. It is possible that the latter reached their nadir, or higher doses of DL-propargylglycine are needed to further reduce their levels, in STZ diabetic rats. Notably, caution is warranted if higher DL-propargylglycine doses are used in future studies in STZ rats because the employed dose reduced the BW and HW in diabetic, but not in non-diabetic rats (Table 1). Importantly, DL-propargylglycine abrogation of the observed effects of moxonidine implicates CSE/H_2S in the favorable cardiovascular and glycemic effects conferred by moxonidine in diabetic rats.

5. Conclusions

The present pharmacological and biochemical findings support a mechanistic role for the CSE/H_2S pathway in the salutary cardiovascular and glycemic effects of moxonidine in STZ diabetic rats. These findings support and extend current views that suppressed endogenous H_2S (CSE expression and activity) is implicated in cardiovascular anomalies associated with hypertension (Ahmad et al., 2012) and diabetes (Jain et al., 2010). Further, our novel findings suggest important roles for adiponectin elevation, and DAPK3 inhibition, in the CSE/H_2S-dependent improvements of cardiovascular function and glycemic control conferred by imidazoline I_1 receptor activation in diabetic rats (Fig. 9). Finally, the current findings yield new insight into the CSE/H_2S-adiponectin pathway as a molecular target for new therapeutics that can concurrently improve glycemic control and cardiovascular function in diabetes.

Acknowledgments

Funding

Supported by Zagazig Faculty of Pharmacy via a scholarship provided by the Egyptian Government (Scholarships Missions Program, Ministry of Higher Education) to Shaimaa S. Elsayed and partially by NIH RO1 AA14441-09 (A. A).

The authors appreciate the technical assistance provided by Ms. Kui Sun

List of Standard Abbreviations

LV +dp/dt$_{max}$	Maximum rate of left ventricle pressure rise
BGL	Blood glucose level
BP	Blood pressure
BRS	Baroreflex sensitivity
CSE	Cystathionine-γ-lyase
DAPK3	Death associated protein kinase-3
ERK	Extracellular signal-regulated kinase
HR	Heart rate
HW/BW	Heart weight/Body weight
MAP	Mean arterial pressure
MAPK	Mitogen activated protein kinase
OGTT	Oral glucose tolerance test
SHR	Spontaneously hypertensive rats
STZ	Streptozotocin

Reference List

Abdel-Rahman AA. Aortic baroreceptors exert a tonically active restraining influence on centrally mediated depressor responses. J Cardiovasc Pharmacol. 1992; 19:233–245. [PubMed: 1376793]

Abe T, Ohga Y, Tabayashi N, Kobayashi S, Sakata S, Misawa H, Tsuji T, Kohzuki H, Suga H, Taniguchi S, Takaki M. Left ventricular diastolic dysfunction in type 2 diabetes mellitus model rats. Am J Physiol Heart Circ Physiol. 2002; 282:H138–148. [PubMed: 11748057]

Aceros H, Farah G, Cobos-Puc L, Stabile AM, Noiseux N, Mukaddam-Daher S. Moxonidine improves cardiac structure and performance in SHR through inhibition of cytokines, p38 MAPK and Akt. Br J Pharmacol. 2011; 164:946–957. [PubMed: 21426316]

Ahmad FU, Sattar MA, Rathore HA, Abdullah MH, Tan S, Abdullah NA, Johns EJ. Exogenous hydrogen sulfide (H2S) reduces blood pressure and prevents the progression of diabetic nephropathy in spontaneously hypertensive rats. Ren Fail. 2012; 34:203–210. [PubMed: 22229751]

Akiyama S, Katsumata S, Suzuki K, Ishimi Y, Wu J, Uehara M. Dietary hesperidin exerts hypoglycemic and hypolipidemic effects in streptozotocin-induced marginal type 1 diabetic rats. J Clin Biochem Nutr. 2010; 46:87–92. [PubMed: 20104270]

Bing C, King P, Pickavance L, Brown M, Ziegler D, Kaan E, Williams G. The effect of moxonidine on feeding and body fat in obese Zucker rats: role of hypothalamic NPY neurones. Br J Pharmacol. 1999; 127:35–42. [PubMed: 10369453]

Borges GR, de Oliveira M, Salgado HC, Fazan R Jr. Myocardial performance in conscious streptozotocin diabetic rats. Cardiovasc Diabetol. 2006; 5:26. [PubMed: 17144912]

Bunag RD, Tomita T, Sasaki S. Streptozotocin diabetic rats are hypertensive despite reduced hypothalamic responsiveness. Hypertension. 1982; 4:556–565. [PubMed: 6218080]

Cao J, Vecoli C, Neglia D, Tavazzi B, Lazzarino G, Novelli M, Masiello P, Wang YT, Puri N, Paolocci N, L'Abbate A, Abraham NG. Cobalt-Protoporphyrin Improves Heart Function by Blunting Oxidative Stress and Restoring NO Synthase Equilibrium in an Animal Model of Experimental Diabetes. Front Physiol. 2012; 3:160. [PubMed: 22675305]

Chen CT, Chen W, Chung HH, Cheng KC, Yeh CH, Cheng JT. Activation of imidazoline I-2B receptor by metformin to increase glucose uptake in skeletal muscle. Horm Metab Res. 2011; 43:708–713. [PubMed: 21932175]

Ebinc H, Ozkurt ZN, Ebinc FA, Ucardag D, Caglayan O, Yilmaz M. Effects of sympatholytic therapy with moxonidine on serum adiponectin levels in hypertensive women. J Int Med Res. 2008; 36:80–87. [PubMed: 18230271]

El-Ayoubi R, Gutkowska J, Regunathan S, Mukaddam-Daher S. Imidazoline receptors in the heart: characterization, distribution, and regulation. J Cardiovasc Pharmacol. 2002; 39:875–883. [PubMed: 12021582]

El-Ayoubi R, Menaouar A, Gutkowska J, Mukaddam-Daher S. Imidazoline receptors but not alpha 2-adrenoceptors are regulated in spontaneously hypertensive rat heart by chronic moxonidine treatment. J Pharmacol Exp Ther. 2004; 310:446–451. [PubMed: 15075383]

El-Mas MM, Abdel-Rahman AA. Nongenomic effects of estrogen mediate the dose-related myocardial oxidative stress and dysfunction caused by acute ethanol in female rats. American journal of physiology Am J Physiol Endocrinol Metab. 2014; 306:E740–747.

Elrod JW, Calvert JW, Morrison J, Doeller JE, Kraus DW, Tao L, Jiao X, Scalia R, Kiss L, Szabo C, Kimura H, Chow CW, Lefer DJ. Hydrogen sulfide attenuates myocardial ischemia-reperfusion injury by preservation of mitochondrial function. Proc Natl Acad Sci U S A. 2007; 104:15560–15565. [PubMed: 17878306]

Erejuwa OO, Sulaiman SA, Wahab MS, Sirajudeen KN, Salleh MS, Gurtu S. Differential responses to blood pressure and oxidative stress in streptozotocin-induced diabetic Wistar-Kyoto rats and spontaneously hypertensive rats: effects of antioxidant (honey) treatment. Int J Mol Sci. 2011; 12:1888–1907. [PubMed: 21673929]

Ernsberger P, Ishizuka T, Liu S, Farrell CJ, Bedol D, Koletsky RJ, Friedman JE. Mechanisms of antihyperglycemic effects of moxonidine in the obese spontaneously hypertensive Koletsky rat (SHROB). J Pharmacol Exp Ther. 1999; 288:139–147. [PubMed: 9862764]

Esler M, Straznicky N, Eikelis N, Masuo K, Lambert G, Lambert E. Mechanisms of sympathetic activation in obesity-related hypertension. Hypertension. 2006; 48:787–796. [PubMed: 17000932]

Frankenfeld SP, de Oliveira LP, Ignacio DL, Coelho RG, Mattos MN, Ferreira AC, Carvalho DP, Fortunato RS. Nandrolone decanoate inhibits gluconeogenesis and decreases fasting glucose in Wistar male rats. J Endocrinol. 2014; 220:143–153. [PubMed: 24403377]

Ganguly PK, Dhalla KS, Innes IR, Beamish RE, Dhalla NS. Altered norepinephrine turnover and metabolism in diabetic cardiomyopathy. Circ Res. 1986; 59:684–693. [PubMed: 3815759]

Gupta S, Sharma B. Pharmacological modulation of I(1)-imidazoline and alpha2-adrenoceptors in sub acute brain ischemia induced vascular dementia. Eur J Pharmacol. 2014; 723:80–90. [PubMed: 24333661]

Hamilton CA, Jardine E, Reid JL. Down-regulation of imidazoline sites in rabbit kidney. Eur J Pharmacol. 1993; 243:95–97. [PubMed: 7902815]

Henriksen EJ, Jacob S, Fogt DL, Youngblood EB, Godicke J. Antihypertensive agent moxonidine enhances muscle glucose transport in insulin-resistant rats. Hypertension. 1997; 30:1560–1565. [PubMed: 9403583]

Honda N, Hirooka Y, Ito K, Matsukawa R, Shinohara K, Kishi T, Yasukawa K, Utsumi H, Sunagawa K. Moxonidine-induced central sympathoinhibition improves prognosis in rats with hypertensive heart failure. J Hypertens. 2013; 31:2300–2308. discussion 2308. [PubMed: 24096260]

Hu N, Dong M, Ren J. Hydrogen sulfide alleviates cardiac contractile dysfunction in an Akt2-knockout murine model of insulin resistance: role of mitochondrial injury and apoptosis. Am J Physiol Regul Integr Comp Physiol. 2014; 306:R761–771. [PubMed: 24622975]

Hua W, Chen Q, Gong F, Xie C, Zhou S, Gao L. Cardioprotection of H2S by downregulating iNOS and upregulating HO-1 expression in mice with CVB3-induced myocarditis. Life Sci. 2013; 93:949–954. [PubMed: 24140888]

Huang J, Wang D, Zheng J, Huang X, Jin H. Hydrogen sulfide attenuates cardiac hypertrophy and fibrosis induced by abdominal aortic coarctation in rats. Mol Med Rep. 2012; 5:923–928. [PubMed: 22245911]

Ibrahim MA, Kanzaki T, Yamagata S, Satoh N, Ueda S. Effect of diabetes on aortic nitric oxide synthesis in spontaneously hypertensive rats; does captopril modulate this effect? Life Sci. 2005; 77:1003–1014. [PubMed: 15890370]

Jain SK, Bull R, Rains JL, Bass PF, Levine SN, Reddy S, McVie R, Bocchini JA. Low levels of hydrogen sulfide in the blood of diabetes patients and streptozotocin-treated rats causes vascular inflammation? Antioxid Redox Signal. 2010; 12:1333–1337. [PubMed: 20092409]

Jain SK, Micinski D, Lieblong BJ, Stapleton T. Relationship between hydrogen sulfide levels and HDL-cholesterol, adiponectin, and potassium levels in the blood of healthy subjects. Atherosclerosis. 2012; 225:242–245. [PubMed: 22989474]

Jiang Y, Steinle JJ. Regulation of IRS-2 signaling by IGF-1 receptor in the diabetic rat heart. Can J Physiol Pharmacol. 2010; 88:553–561. [PubMed: 20555424]

Lee SD, Kuo WW, Ho YJ, Lin AC, Tsai CH, Wang HF, Kuo CH, Yang AL, Huang CY, Hwang JM. Cardiac Fas-dependent and mitochondria-dependent apoptosis in ovariectomized rats. Maturitas. 2008; 61:268–277. [PubMed: 18951737]

Leung JY, Pang CC. Effects of nimesulide, a selective COX-2 inhibitor, on cardiovascular function in 2 rat models of diabetes. J Cardiovasc Pharmacol. 2014; 64:79–86. [PubMed: 24621649]

Li CJ, Lv L, Li H, Yu DM. Cardiac fibrosis and dysfunction in experimental diabetic cardiomyopathy are ameliorated by alpha-lipoic acid. Cardiovasc Diabetol. 2012; 11:73. [PubMed: 22713251]

Li G, Abdel-Rahman AA. Direct evidence for imidazoline (I1) receptor modulation of ethanol action on norepinephrine-containing neurons in the rostral ventrolateral medulla in conscious spontaneously hypertensive rats. Alcohol Clin Exp Res. 2007; 31:684–693. [PubMed: 17374048]

Liang B, Guo Z, Xie F, Zhao A. Antihyperglycemic and antihyperlipidemic activities of aqueous extract of Hericium erinaceus in experimental diabetic rats. BMC Complement Altern Med. 2013; 13:253. [PubMed: 24090482]

Liu Y, Palanivel R, Rai E, Park M, Gabor TV, Scheid MP, Xu A, Sweeney G. Adiponectin stimulates autophagy and reduces oxidative stress to enhance insulin sensitivity during high-fat diet feeding in mice. Diabetes. 2015; 64:36–48. [PubMed: 25071026]

Manna P, Jain SK. Vitamin D up-regulates glucose transporter 4 (GLUT4) translocation and glucose utilization mediated by cystathionine-gamma-lyase (CSE) activation and H2S formation in 3T3L1 adipocytes. J Biol Chem. 2012; 287:42324–42332. [PubMed: 23074218]

Milan A, Caserta MA, Del Colle S, Dematteis A, Morello F, Rabbia F, Mulatero P, Pandian NG, Veglio F. Baroreflex sensitivity correlates with left ventricular morphology and diastolic function in essential hypertension. J Hypertens. 2007; 25:1655–1664. [PubMed: 17620963]

Mukaddam-Daher S. An “I” on cardiac hypertrophic remodelling: imidazoline receptors and heart disease. Can J Cardiol. 2012; 28:590–598. [PubMed: 22483786]

Mukaddam-Daher S, Menaouar A, Paquette PA, Jankowski M, Gutkowska J, Gillis MA, Shi YF, Calderone A, Tardif JC. Hemodynamic and cardiac effects of chronic eprosartan and moxonidine therapy in stroke-prone spontaneously hypertensive rats. Hypertension. 2009; 53:775–781. [PubMed: 19273740]

Musial DC, da Silva ED Junior, da Silva RM, Miranda-Ferreira R, Lima-Landman MT, Jurkiewicz A, Garcia AG, Jurkiewicz NH. Increase of angiotensin-converting enzyme activity and peripheral sympathetic dysfunction could contribute to hypertension development in streptozotocin-induced diabetic rats. Diab Vasc Dis Res. 2013; 10:498–504. [PubMed: 23975725]

National Research Council (U.S.). Committee for the Update of the Guide for the Care and Use of Laboratory Animals., Institute for Laboratory Animal Research (U.S.), National Academies Press (U.S.). Guide for the care and use of laboratory animals. 8. National Academies Press; Washington, D.C: 2011.

Okamoto M, Yamaoka M, Takei M, Ando T, Taniguchi S, Ishii I, Tohya K, Ishizaki T, Niki I, Kimura T. Endogenous hydrogen sulfide protects pancreatic beta-cells from a high-fat diet-induced glucotoxicity and prevents the development of type 2 diabetes. Biochem Biophys Res Commun. 2013; 442:227–233. [PubMed: 24246677]

Patel KP, Mayhan WG, Bidasee KR, Zheng H. Enhanced angiotensin II-mediated central sympathoexcitation in streptozotocin-induced diabetes: role of superoxide anion. American journal of physiology Am J Physiol Regul Integr Comp Physiol. 2011; 300:R311–320.

Patel KP, Zhang PL. Baroreflex function in streptozotocin (STZ) induced diabetic rats. Diabetes Res Clin Pract. 1995; 27:1–9. [PubMed: 7781488]

Pieper GM. Review of alterations in endothelial nitric oxide production in diabetes: protective role of arginine on endothelial dysfunction. Hypertension. 1998; 31:1047–1060. [PubMed: 9576113]

Qi Y, Xu Z, Zhu Q, Thomas C, Kumar R, Feng H, Dostal DE, White MF, Baker KM, Guo S. Myocardial loss of IRS1 and IRS2 causes heart failure and is controlled by p38alpha MAPK during insulin resistance. Diabetes. 2013; 62:3887–3900. [PubMed: 24159000]

Rosen P, Ohly P, Gleichmann H. Experimental benefit of moxonidine on glucose metabolism and insulin secretion in the fructose-fed rat. J Hypertens Suppl. 1997; 15:S31–38. [PubMed: 9050983]

Saini AS, Taliyan R, Sharma PL. Protective effect and mechanism of Ginkgo biloba extract-EGb 761 on STZ-induced diabetic cardiomyopathy in rats. Pharmacogn Mag. 2014; 10:172–178. [PubMed: 24914284]

Shaltout HA, Abdel-Rahman AA. Mechanism of fatty acids induced suppression of cardiovascular reflexes in rats. J Pharmacol Exp Ther. 2005; 314:1328–1337. [PubMed: 15937146]

Shida T, Nozawa T, Sobajima M, Ihori H, Matsuki A, Inoue H. Fluvastatin-induced reduction of oxidative stress ameliorates diabetic cardiomyopathy in association with improving coronary microvasculature. Heart Vessels. 2014; 29:532–541. [PubMed: 23979266]

Stabile AM, Aceros H, Stockmeyer K, Abdel Rahman AA, Noiseux N, Mukaddam-Daher S. Functional and molecular effects of imidazoline receptor activation in heart failure. Life Sci. 2011; 88:493–503. [PubMed: 21277868]

Stipanuk MH, Beck PW. Characterization of the enzymic capacity for cysteine desulphhydration in liver and kidney of the rat. The Biochemical journal. 1982; 206:267–277. [PubMed: 7150244]

Streeter E, Ng HH, Hart JL. Hydrogen sulfide as a vasculoprotective factor. Med Gas Res. 2013; 3:9. [PubMed: 23628084]

Turcani M. Biphasic dose-dependent modulation of cardiac parasympathetic activity by moxonidine, an imidazoline I1-receptor agonist. J Cardiovasc Pharmacol. 2008; 52:524–535. [PubMed: 19034032]

Usui T, Okada M, Hara Y, Yamawaki H. Death-associated protein kinase 3 mediates vascular inflammation and development of hypertension in spontaneously hypertensive rats. Hypertension. 2012; 60:1031–1039. [PubMed: 22868392]

Van Kerckhoven R, van Veen TA, Boomsma F, Saxena PR, Schoemaker RG. Chronic administration of moxonidine suppresses sympathetic activation in a rat heart failure model. Eur J Pharmacol. 2000; 397:113–120. [PubMed: 10844105]

Velasco-Xolalpa ME, Barragan-Iglesias P, Roa-Coria JE, Godinez-Chaparro B, Flores-Murrieta FJ, Torres-Lopez JE, Araiza-Saldana CI, Navarrete A, Rocha-Gonzalez HI. Role of hydrogen sulfide in the pain processing of non-diabetic and diabetic rats. Neuroscience. 2013; 250:786–797. [PubMed: 23830907]

Wang X, Abdel-Rahman AA. Estrogen modulation of eNOS activity and its association with caveolin-3 and calmodulin in rat hearts. American journal of physiology Am J Physiol Heart Circ Physiol. 2002; 282:H2309–2315.

Xue H, Yuan P, Ni J, Li C, Shao D, Liu J, Shen Y, Wang Z, Zhou L, Zhang W, Huang Y, Yu C, Wang R, Lu L. H(2)S inhibits hyperglycemia-induced intrarenal renin-angiotensin system activation via attenuation of reactive oxygen species generation. PloS One. 2013a; 8:e74366. [PubMed: 24058553]

Xue R, Hao DD, Sun JP, Li WW, Zhao MM, Li XH, Chen Y, Zhu JH, Ding YJ, Liu J, Zhu YC. Hydrogen sulfide treatment promotes glucose uptake by increasing insulin receptor sensitivity and ameliorates kidney lesions in type 2 diabetes. Antioxid Redox Signal. 2013b; 19:5–23. [PubMed: 23293908]

Yamakawa T, Tanaka S, Numaguchi K, Yamakawa Y, Motley ED, Ichihara S, Inagami T. Involvement of Rho-kinase in angiotensin II-induced hypertrophy of rat vascular smooth muscle cells. Hypertension. 2000; 35:313–318. [PubMed: 10642317]

Yan H, Du J, Tang C. The possible role of hydrogen sulfide on the pathogenesis of spontaneous hypertension in rats. Biochem Biophys Res Commun. 2004; 313:22–27. [PubMed: 14672692]

Zheng H, Mayhan WG, Bidasee KR, Patel KP. Blunted nitric oxide-mediated inhibition of sympathetic nerve activity within the paraventricular nucleus in diabetic rats. Am J Physiol Regul Integr Comp Physiol. 2006; 290:R992–R1002. [PubMed: 16322352]

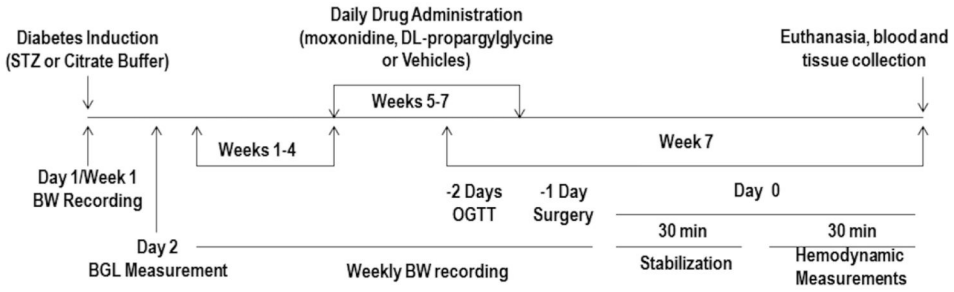

Fig. 1.

A schematic presentation of diabetes induction, pharmacologic intervention, and the biochemical and molecular studies conducted to investigate the glycemic and cardiovascular effects of moxonidine (2 or 6 mg/kg/day, p.o) in diabetic male Wistar rats in the absence or presence of H_2S-synthesis inhibitor, DL-propargylglycine (37.5 mg/kg/day, i.p) during the last 3 weeks of the experiment. STZ, streptozotocin; BW, body weight; BGL, blood glucose level; OGTT, oral glucose tolerance test.

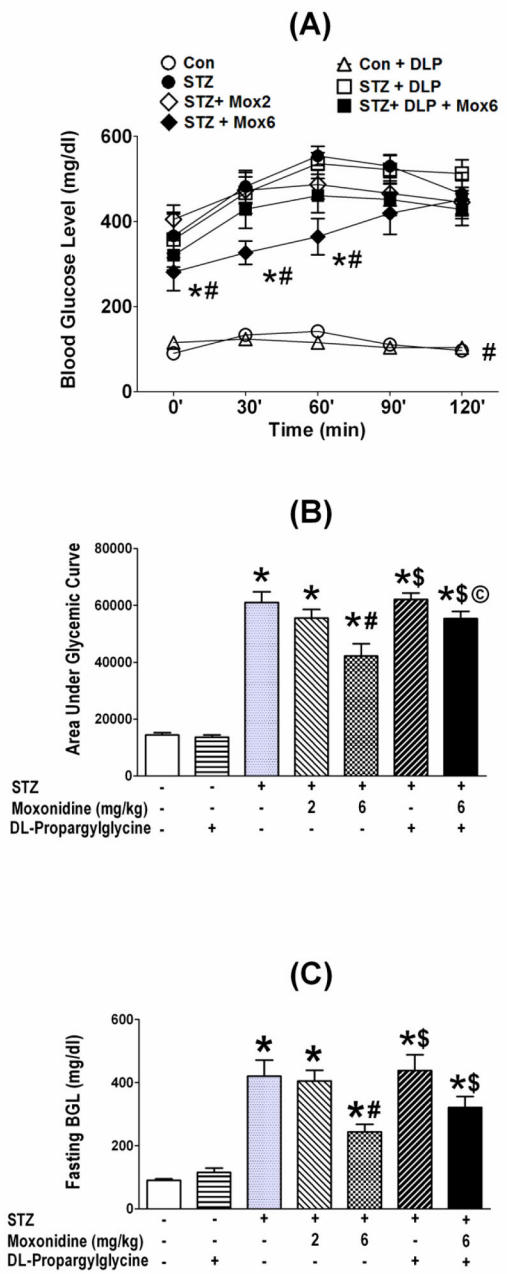

Fig. 2.

Effect of 3-week treatment with moxonidine (2 or 6 mg/kg/day for 3 weeks; gavage; Mox 2 or Mox 6), administered 4 weeks after diabetes induction, on the glycemic control presented as glycemic tolerance (A) and, as area under glycemic curve (B) and on fasting blood glucose (C) and, in STZ diabetic male Wistar rats. Shown also are the effects of DL-propargylglycine, DLP (37.5 mg/kg/day; i.p) administered alone in non-diabetic (Con) or STZ-diabetic rats or in combination with moxonidine (6 mg/kg/day) in diabetic rats. Values are means ± S.E.M. (n=5–8 rats/group); * P <0.05 versus vehicle treated non-diabetic rats, # P <0.05 versus vehicle-treated diabetic rats, $ P<0.05 versus DL-propargylglycine treated nondiabetic rats and © P< 0.05 versus moxonidine (6 mg/kg) treated diabetic rats.

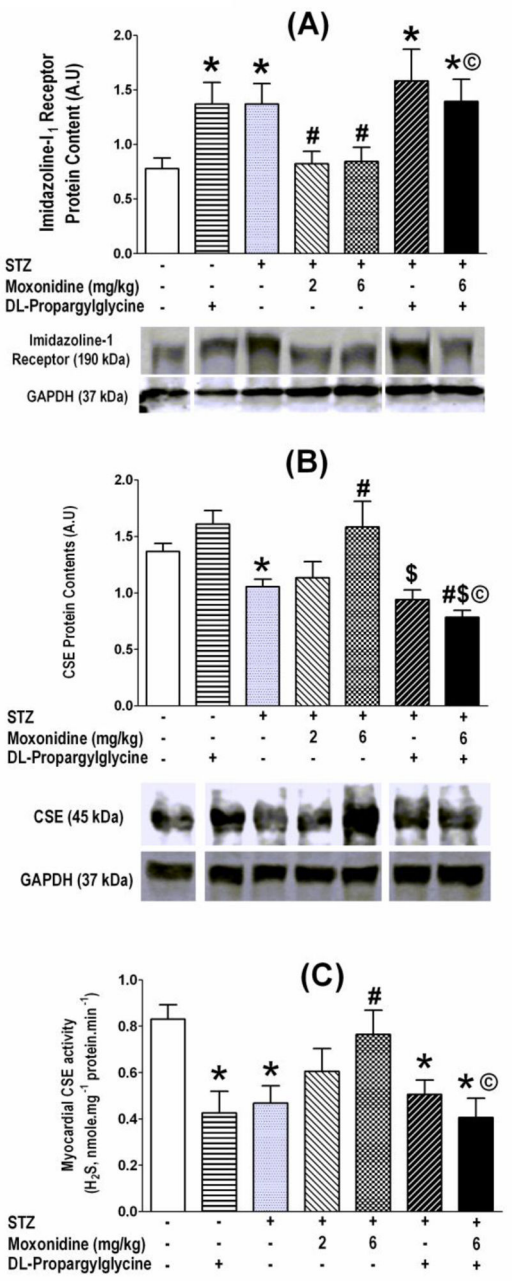

Fig. 3.

Moxonidine (2 or 6 mg/kg/day for 3 weeks; gavage), administered 4 weeks after diabetes induction, ameliorated the diabetes-induced imidazoline I_1 receptor upregulation (A), reductions in CSE expression (B) and activity (C) in the myocardium of STZ diabetic male Wistar rats. Shown also are the effects of DL-propargylglycine (37.5 mg/kg/day; i.p) administered alone in non-diabetic or diabetic male Wistar rats or in combination with moxonidine (6 mg/kg/day) in diabetic rats. Values are means ± S.E.M. (n=5–8 rats/group); * P <0.05 versus vehicle treated non-diabetic rats, # P <0.05 versus vehicle-treated diabetic rats, $ P<0.05 versus DL-propargylglycine treated nondiabetic rats and © P< 0.05 versus moxonidine (6 mg/kg) treated diabetic rats. Molecular weights of proteins were given in

kDa, and splicing gel lanes was needed due to exclusion of some treatment groups from the study.

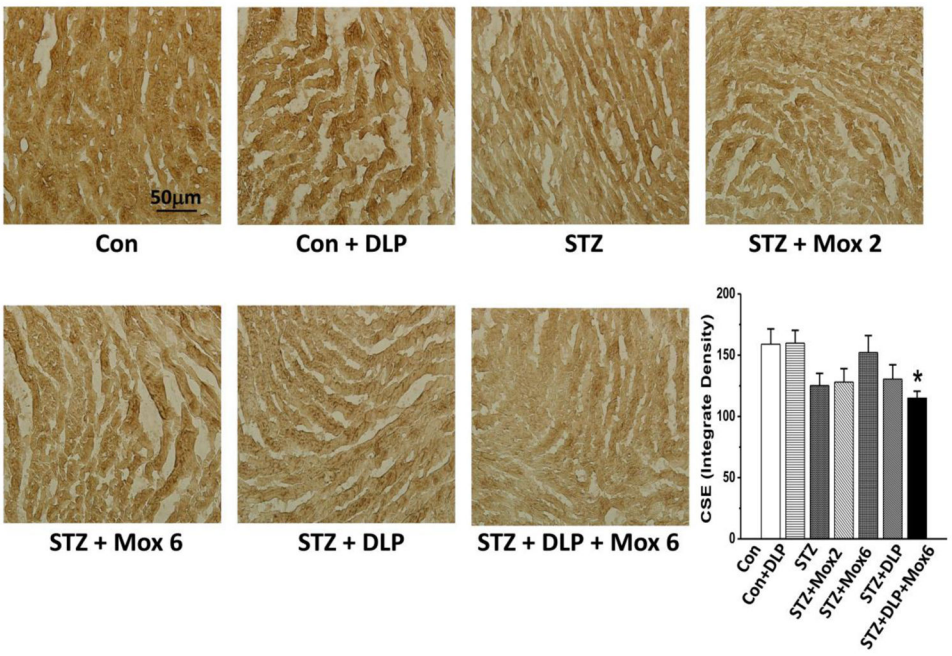

Fig. 4.

Immunohistochemical detection of cystathionine-γ lyase (CSE) in ventricular myocytes of STZ-diabetic male Wistar rats treated with moxonidine (2 or 6 mg/kg/day for 3 weeks; gavage; Mox 2 or Mox 6), administered 4 weeks after diabetes induction. Shown also are the effects of DL-propargylglycine, DLP (37.5 mg/kg/day; i.p) administered alone in non-diabetic (Con) or STZ-diabetic male Wistar rats or in combination with moxonidine (6 mg/kg/day) in STZ-diabetic rats. Values are means ± S.E.M. (n=5–8 rats/group); * P <0.05 versus vehicle treated non-diabetic rats.

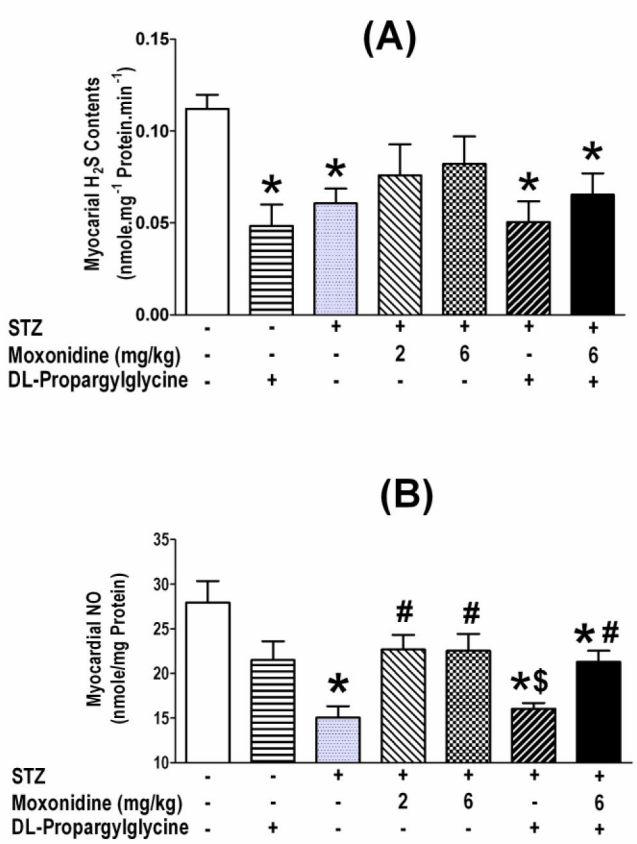

Fig. 5.

Moxonidine (2 or 6 mg/kg/day for 3 weeks; gavage), administered 4 weeks after diabetes induction, ameliorated the reductions in hydrogen sulfide (H_2S) levels (A) and nitric oxide (NO) levels (B) in the myocardium of STZ diabetic male Wistar rats. Shown also are the effects of DL-propargylglycine (37.5 mg/kg/day; i.p) administered alone in non-diabetic or diabetic male Wistar rats or in combination with moxonidine (6 mg/kg/day) in diabetic rats. Values are means ± S.E.M. (n=5–8 rats/group); * P <0.05 versus vehicle treated non-diabetic rats, # P <0.05 versus vehicle-treated diabetic rats, $ P<0.05 versus DL-propargylglycine treated nondiabetic rats and © P< 0.05 versus moxonidine (6 mg/kg) treated diabetic rats.

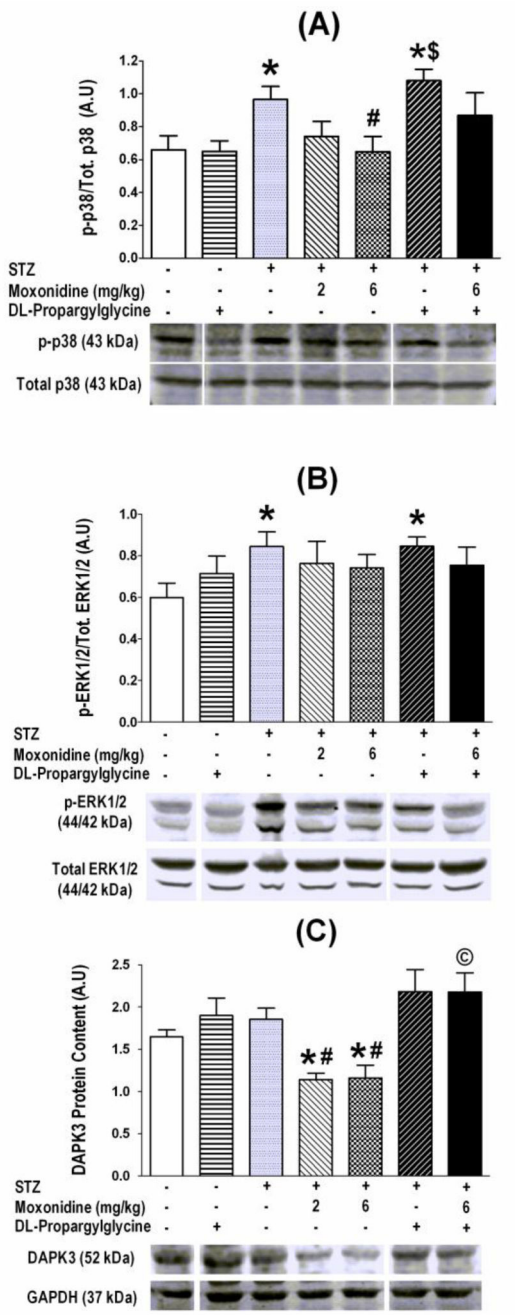

Fig. 6.

Moxonidine (2 or 6 mg/kg/day for 3 weeks; gavage), administered 4 weeks after diabetes induction, ameliorated the enhanced phosphorylation of p38 (A) and ERK1/2 (B) and suppressed DAPK3 expression (C) in STZ diabetic male Wistar rats. Shown also are the effects of DL-propargylglycine (37.5 mg/kg/day; i.p) administered alone in non-diabetic or diabetic male Wistar rats or in combination with moxonidine (6 mg/kg/day) in diabetic rats. Values are means ± S.E.M. (n=5–8 rats/group); * P <0.05 versus vehicle treated non-diabetic rats, # P <0.05 versus vehicle-treated diabetic rats, $ P<0.05 versus DL-propargylglycine treated nondiabetic rats and © P< 0.05 versus moxonidine (6 mg/kg) treated diabetic rats.

Molecular weights of proteins were given in kDa, and representative blots for a particular protein in treatment and control groups were all run on the same gel; whenever the random order of the blots necessitated splicing gel lanes to present representative blots, this was identified by the gap in the presented blots.

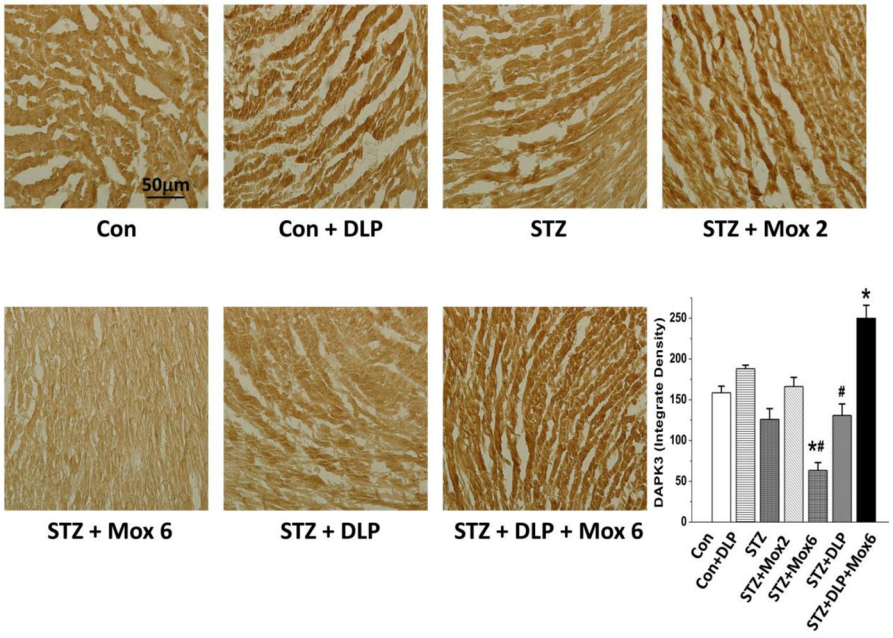

Fig. 7.

Immunohistochemical detection of Death Associated Protein Kinase-3 (DAPK-3) in ventricular myocytes of STZ-diabetic male Wistar rats treated with moxonidine (2 or 6 mg/kg/day for 3 weeks; gavage; Mox 2 or Mox 6), administered 4 weeks after diabetes induction. Shown also are the effects of DL-propargylglycine, DLP (37.5 mg/kg/day; i.p) administered alone in non-diabetic (Con) or STZ-diabetic male Wistar rats or in combination with moxonidine (6 mg/kg/day; Mox 6) in STZ-diabetic rats. Values are means ± S.E.M. (n=5–8 rats/group); * $P<0.05$ versus vehicle treated non-diabetic rats, $^{\#}$ $P<0.05$ versus vehicle-treated diabetic rats.

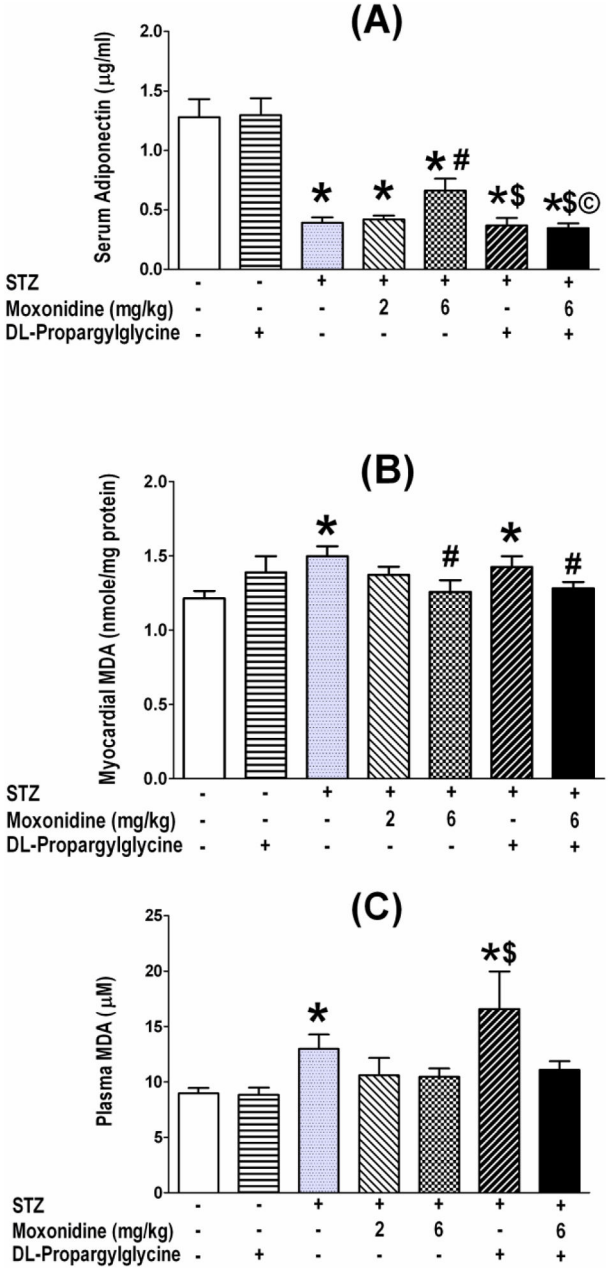

Fig. 8.

Amelioration by moxonidine (2 or 6 mg/kg/day for 3 weeks; gavage), administered 4 weeks after diabetes induction, of the reduction in serum adiponectin (A) and the elevations in plasma (B) and myocardial (C) malondialdehyde (MDA) in STZ diabetic male Wistar rats. Shown also are the effects of DL-propargylglycine (37.5 mg/kg/day; i.p) administered alone in non-diabetic or diabetic male Wistar rats or in combination with moxonidine (6 mg/kg/day) in diabetic rats. Values are means ± S.E.M. (n=5–8 rats/group); * $P<0.05$ versus vehicle treated non-diabetic rats, $^{\#}$ $P<0.05$ versus vehicle-treated diabetic rats, $^{\$}$ $P<0.05$ versus DL-propargylglycine treated nondiabetic rats and $^{©}$ $P< 0.05$ versus moxonidine (6 mg/kg) treated diabetic rats.

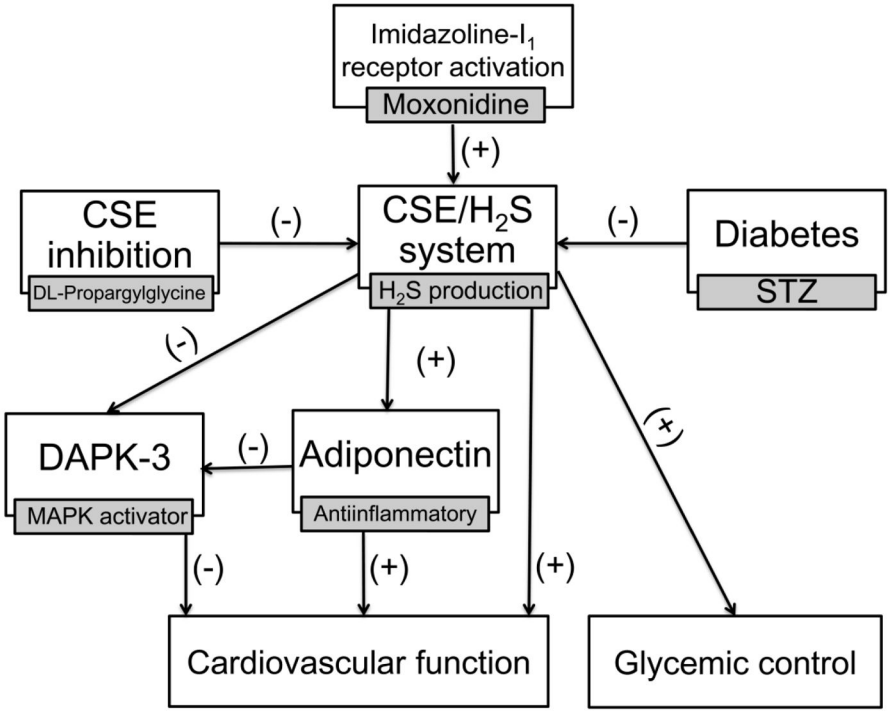

Fig. 9.

Suggested mechanisms for the improvement of cardiovascular function and glycemic control conferred by imidazoline I_1 receptor activation in diabetic rats based on: (i) moxonidine ability to improve myocardial function (Table 2) and glycemic control (Fig. 2) along with reversing the reductions in myocardial cystathionine-γ lyase (CSE) expression/activity/H_2S level (Figs. 3B, C and 5A) and circulating adiponectin (Fig. 8A); (ii) moxonidine-evoked suppression of Death Associated Protein Kinase-3 (DAPK-3) and mitogen activated protein kinase (MAPK) phosphorylation (Figs. 6, 7); (iii) abrogation by CSE inhibition (DL-propargylglycine) of the aforementioned biochemical events and the favorable cardiovascular effects and glycemic control elicited by moxonidine in diabetic rats (see text for details).

Table 1

Effects of 3-week treatment with moxonidine (2 or 6 mg/kg/day; gavage), starting 4 week following diabetes induction, on heart weight (HW), body weight (BW) and HW/BW ratio “index of hypertrophy” in STZ diabetic male Wistar rats. Shown also are the effects of DL-propargylglycine alone in non-diabetic and diabetic rats, and in combination with moxonidine (6 mg/kg/day) in diabetic rats.

	Heart weight (HW) (g)	Body weight (BW) (g)	HW/BW Ratio
Nondiabetic + Vehicle (n=8)	1.44 ± 0.07	462.5 ± 19.2	3.113 ± 0.048
Nondiabetic+ DL-Propargylglycine (n=7)	1.33 ± 0.05	432.3 ± 13.6	3.086 ± 0.101
Diabetic + Vehicle (n=8)	1.27 ± 0.02[a]	339.6 ± 12.8[a]	3.854 ± 0.126[a]
Diabetic + Moxonidine (2 mg/kg) (n=8)	1.11 ± 0.05[a, b]	298.5 ± 16.04[a]	3.504 ± 0.188[a]
Diabetic + Moxonidine (6 mg/kg) (n=8)	1.08 ± 0.05[a, b]	315.3 ± 17.9[a]	3.333 ± 0.143[b]
Diabetic + DL-Propargylglycine (n=8)	1.11 ± 0.04[a, b, c]	299.6 ± 14.8[a, c]	3.906 ± 0.186[a, c]
Diabetic + DL-Propargylglycine + Moxonidine (6 mg/kg) (n=8)	0.87 ± 0.052[a, b, c,d]	265.8 ± 12.0 [a, b, c,d]	3.345 ± 0.081[a, b]

Values are means ± S.E.M. (n=7–8 rats/group);

[a] P<0.05 versus vehicle treated non-diabetic rats,

[b] P<0.05 versus vehicle-treated diabetic rats,

[c] P<0.05 versus DL-Propargylglycine treated nondiabetic rats and

[d] P< 0.05 versus moxonidine (6 mg/kg) treated diabetic rats.

Table 2

Effects of 3-week treatment with moxonidine (2 or 6 mg/kg/day; gavage), starting 4 week following diabetes induction, on mean arterial pressure (MAP), heart rate (HR), and myocardial (LV +dp/dt) and baroreflex (BRS; Seq."BRS-SAP" TOTAL) function in STZ diabetic male Wistar rats. Shown also are the effects of DL-propargylglycine alone in non-diabetic and diabetic rats and in combination with moxonidine (6 mg/kg/day) in diabetic rats.

	MAP (mmHg)	HR (bpm)	LV +dp/dt (mmHg/sec)	Seq. (BRS-SAP) TOTAL (ms/mmHg)
Nondiabetic + Vehicle (n=8)	95.3 ± 4.3	319.5 ± 11.3	7219 ± 588.3	2.39 ± 0.23
Nondiabetic + DL-Propargylglycine (n=7)	95.8 ± 6.4	326.4 ± 12.6	5315 ± 503.4[a]	2.50 ± 0.29
Diabetic + Vehicle (n=8)	109.9 ± 2.5[a]	338.9 ± 24.5	4709 ± 474.6[a]	1.41 ± 0.23[a]
Diabetic + Moxonidine (2 mg/kg) (n=8)	93.2 ± 3.4[b]	310.6 ± 14.3	6224 ± 537.6[b]	2.79 ± 0.62[b]
Diabetic + Moxonidine (6 mg/kg) (n=8)	71.0 ± 3.3[a, b]	266.1 ± 11.2 [a, b]	6250 ± 413.2[b]	2.18 ± 0.15[b]
Diabetic + DL-Propargylglycine (n=8)	98.1 ± 6.5	333.9 ± 13.9	5211 ± 442.7[a]	3.38 ± 0.36[b]
Diabetic + DL-Propargylglycine + Moxonidine (6 mg/kg) (n=8)	81.7 ± 6.3[b]	294.1 ± 32.5	5172 ± 360.6[a, d]	2.88 ± 0.50[b]

Values are means ± S.E.M. (n=5–8 rats/group);

[a] P<0.05 versus vehicle treated non-diabetic rats,

[b] P<0.05 versus vehicle-treated diabetic rats, and

[d] P< 0.05 versus moxonidine (6 mg/kg) treated diabetic rats.